Supporting information for

Electrochemical Amination of Acetone using Ag as Cathode: Mechanism and Role of Pb Impurities for Hydrogen Transfer

Yani Guan,[a] Justus Kümper,[b] Angelina Cuomo,[c,d] Simran Kumari,[a] Sonja D. Mürtz,[b] Pavlo Nikolaienko,[c] Karl J. J. Mayrhofer,*[c,d] Regina Palkovits*[b,e] and Philippe Sautet*[a,f]

[a] Department of Chemical and Biomolecular Engineering,
University of California Los Angeles,
Los Angeles, CA 90095, USA

[b] Chair of Heterogeneous Catalysis and Technical Chemistry
RWTH Aachen University
Worringerweg 2, 52074 Aachen (Germany)

[c] Helmholtz Institute Erlangen-Nürnberg for Renewable Energy (IET-2)
Forschungszentrum Jülich GmbH
Cauerstr. 1, 91058 Erlangen, Germany

[d] Department of Chemical and Biological Engineering
Friedrich-Alexander University Erlangen-Nürnberg
Cauerstr. 1, 91058 Erlangen, Germany

[e] Institute for a Sustainable Hydrogen Economy (IHE-2), Forschungszentrum Jülich, An der Deutschen Welle 7a,, 52428 Jülich, Germany

[f] Department of Chemistry and Biochemistry,
University of California Los Angeles,
Los Angeles, CA 90095, USA

*k.mayrhofer@fz-juelich.de

*palkovits@itmc.rwth-aachen.de / r.palkovits@fz-juelich.de

*sautet@ucla.edu

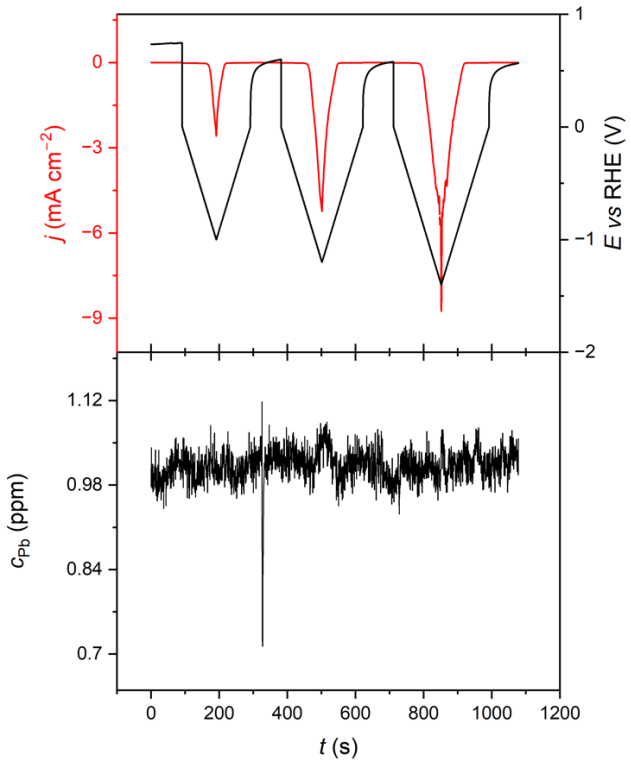

Figure S1. Impact of the applied potential on Pb concentration in the electrolyte, to prove whether Pb is irreversibly deposited on the GC electrode. The electrolyte contained 1 ppm Pb that was introduced as $Pb(NO_3)_2$. No decrease in Pb concentration was measured, illustrating that under these conditions no irreversible deposition was present. Signal at 300 s represents a measurement inaccuracy as it was only measured once and is located between two CV measurements. (Conditions: WE: GC, CE: GC; scan rate: 10 mV s^{-1}; solvent: 0.5 M KH_2PO_4; substrate: acetone: 2.4 M, methylamine: 2.9 M; pH of the final reaction solution: 13).

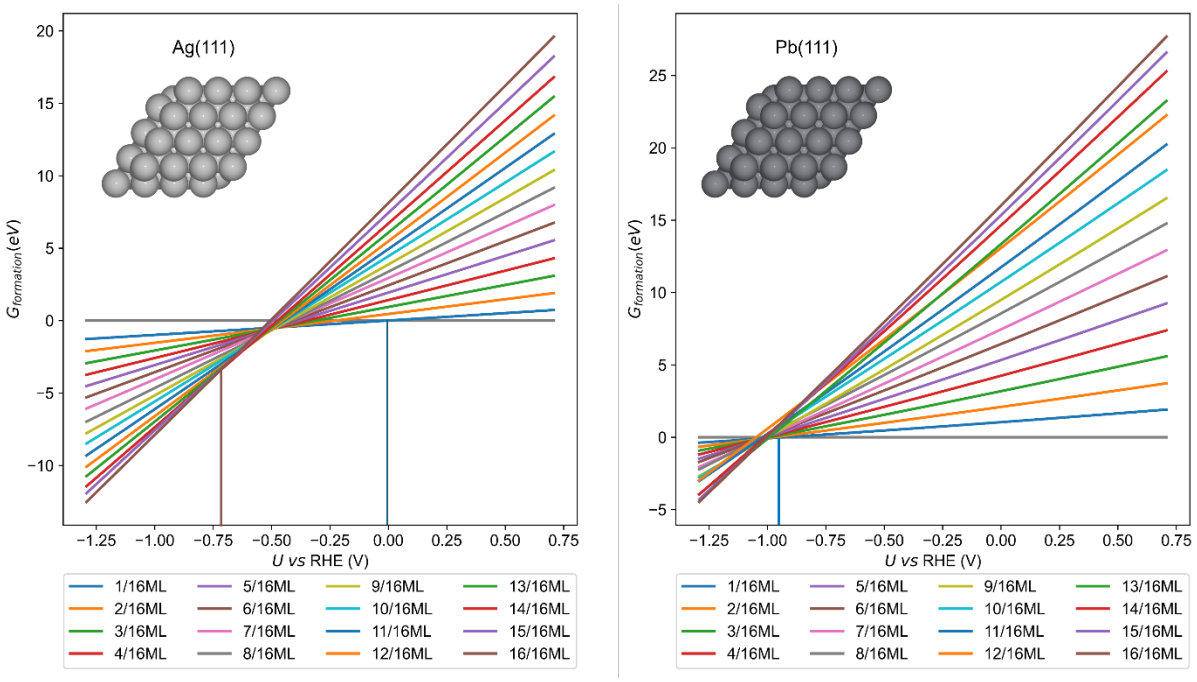

Figure S2. Hydrogen affinity of Ag and Pb, where 4 x 4 Ag (111) and Pb(111) surface were constructed to check the thermodynamic stability of H coverage from 1/16ML to 16/16ML.

To assess the role of hydrogen evolution as a competing side reaction in Pb-mediated electrochemical systems, we systematically investigated HER involving surface-bound Pb–H species by combining thermodynamic analysis, potential-dependent CHE modeling, and explicit-solvent kinetic calculations. Surface-bound Pb hydrides (PbH_4, PbH_3, and PbH_2) were found to form readily under strongly cathodic conditions, serving as key hydrogen reservoirs at the interface. Thermodynamic analysis shows that H–H coupling and hydrogen release from PbH_x species are exergonic across a wide potential window, with the relative stability of hydrides evolving as a function of electrode potential. In particular, higher-order hydrides are favored at moderate cathodic potentials, whereas PbH_2 becomes thermodynamically dominant under more negative conditions, indicating progressive hydride depletion upon hydrogen evolution.

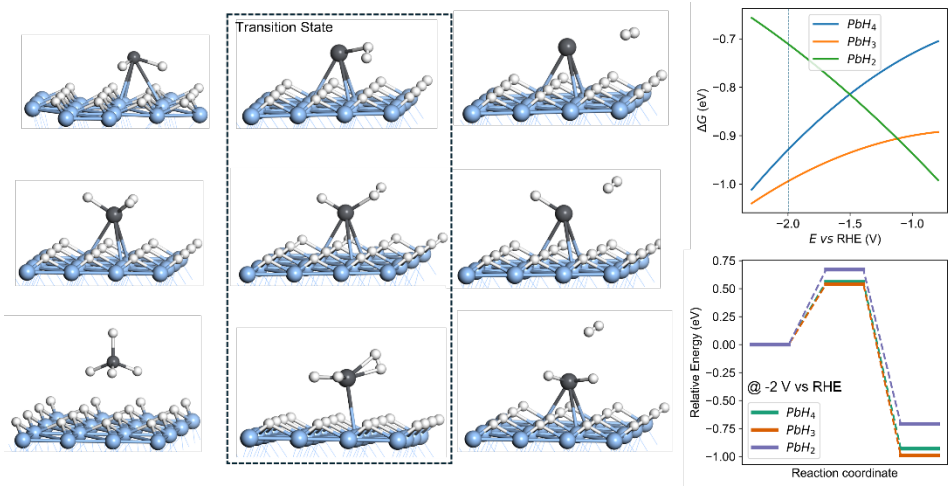

Figure S3. Hydrogen evolution reaction (HER) pathways with surface-bound Pb hydrides (PbH_4, PbH_3, and PbH_2) participating in H–H bond formation

Using the computational hydrogen electrode (CHE) framework, we evaluated a Heyrovsky-type HER pathway in which a proton–electron pair from solution reacts with a surface-bound hydride to form H_2. The resulting potential-dependent free energies reveal that PbH_x species exhibit distinct reactivities toward hydrogen evolution, with PbH_3 displaying the most favorable thermodynamics for H_2 formation, while PbH_4 is comparatively less reactive. These trends reflect differences in Pb–H bond strength and hydrogen chemical potential, highlighting the sensitivity of HER thermodynamics to hydride stoichiometry.

To further validate the kinetic feasibility of HER, we explicitly modeled protonation steps using water clusters to represent the local solvation environment. Water-assisted proton transfer proceeds through a hydrogen-bonded relay mechanism, yielding moderate activation barriers that remain accessible under operating electrochemical conditions. Consistent with the thermodynamic analysis, PbH_3 exhibits the lowest protonation barrier, whereas PbH_4 displays a higher kinetic penalty, indicating that highly hydrogenated Pb centers are kinetically less prone to immediate hydrogen evolution.

Taken together, these results demonstrate that surface-bound Pb–H species can actively participate in hydrogen evolution via both hydride coupling and Heyrovsky-type pathways.

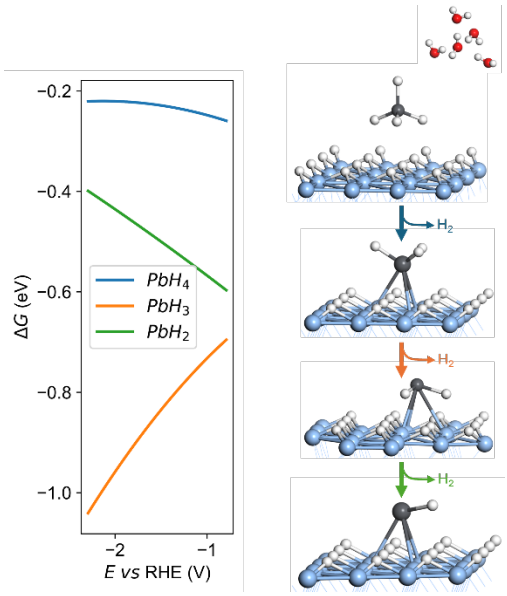

Figure S4. Potential-dependent thermodynamics of Heyrovsky-type HER on Pb–H_x species

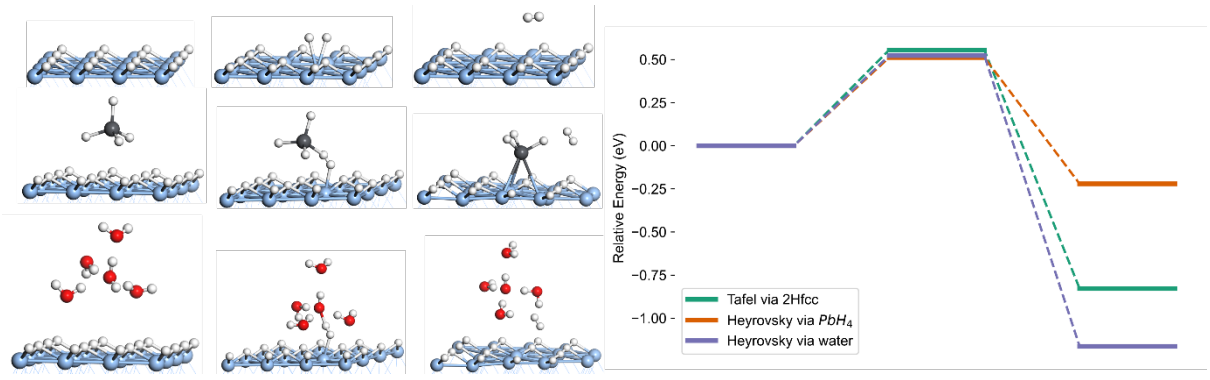

Figure S5. Tafel HER on 16/16 ML Ag (111) surface in green, Heyrovsky HER via solvent water in purple and Heyrovsky-like HER via PbH_4 in orange.

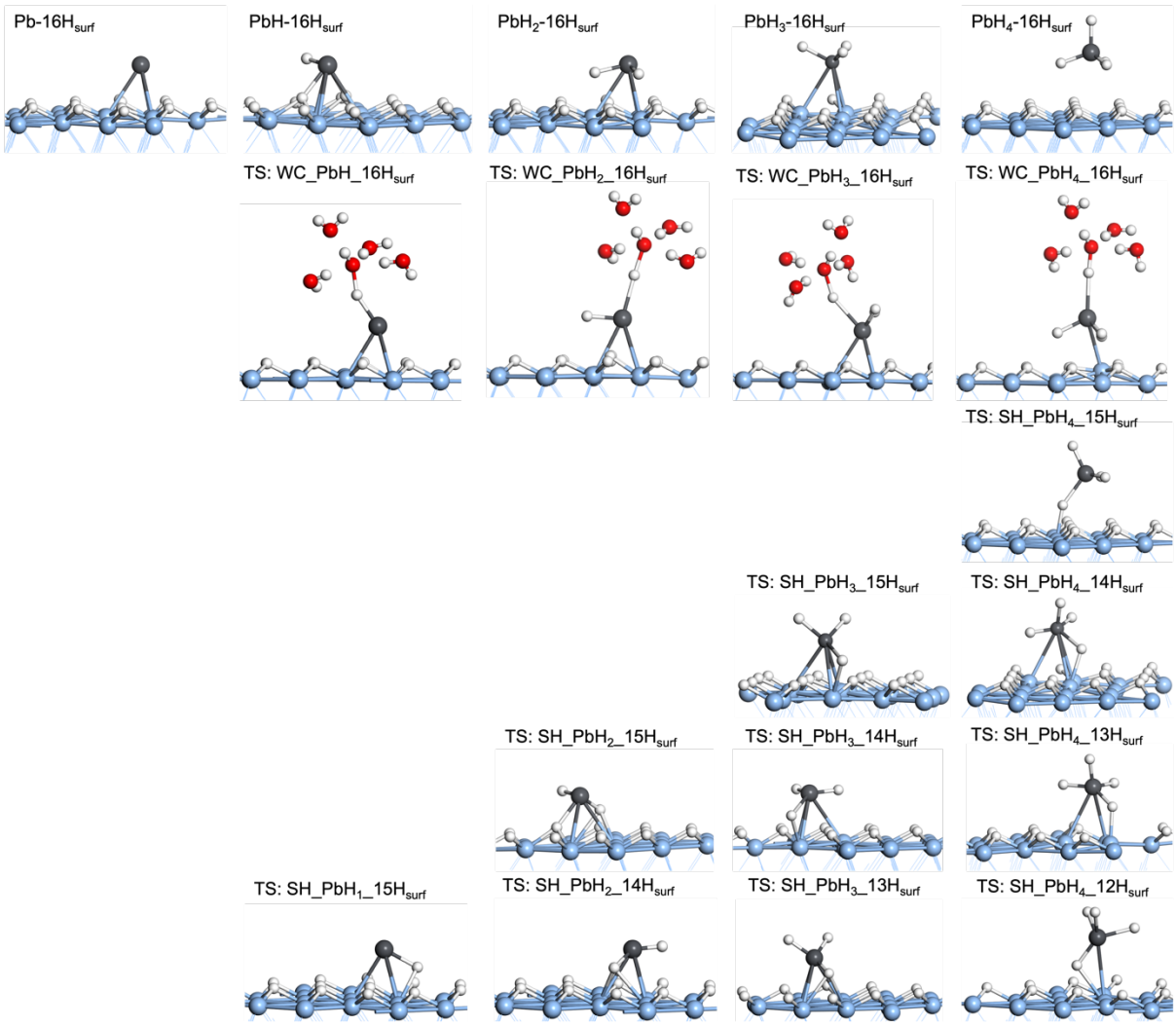

Figure S6. Depicts the structures corresponding to Figure 2d in the main text. The top row shows the optimized Pb hydride species from Pb through PbH_4, and the second row presents the transition-state structures for the proton-coupled electron transfer (PCET) pathway. From the third row onwards, the figure illustrates the transition-state structures for surface-mediated hydrogenation under total hydrogen coverages of 19, 18, 17, and 16 H, respectively.

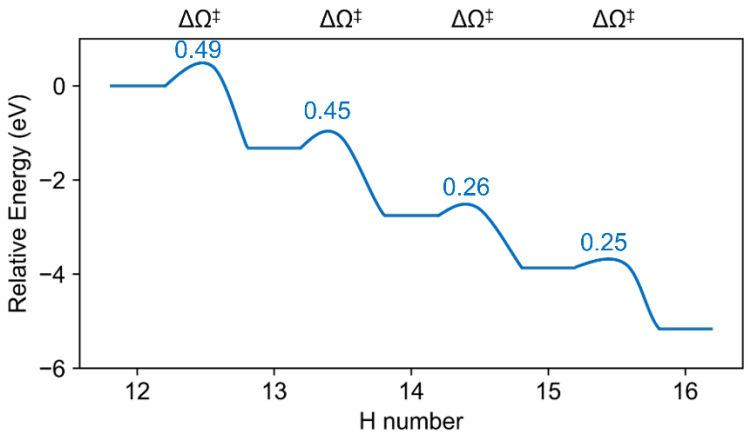

Figure S7. The kinetic profiles of Ag surface replenishment using solvent water cluster.

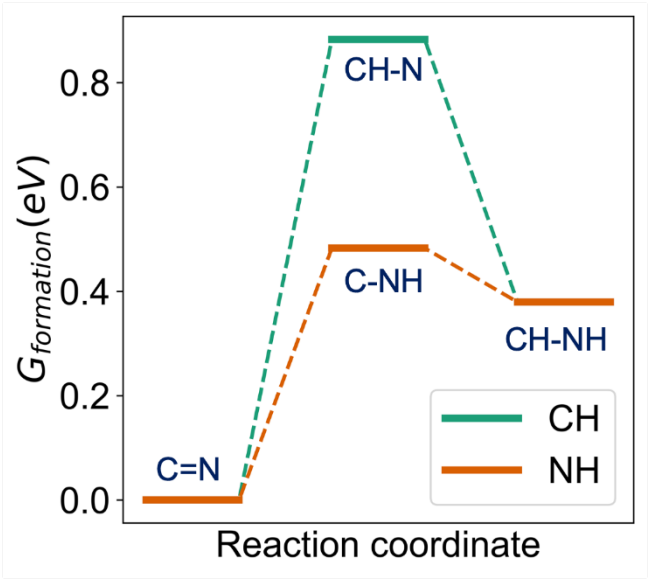

Figure S8. Reaction profiles of imine hydrogenation by PbH_2 in solution.

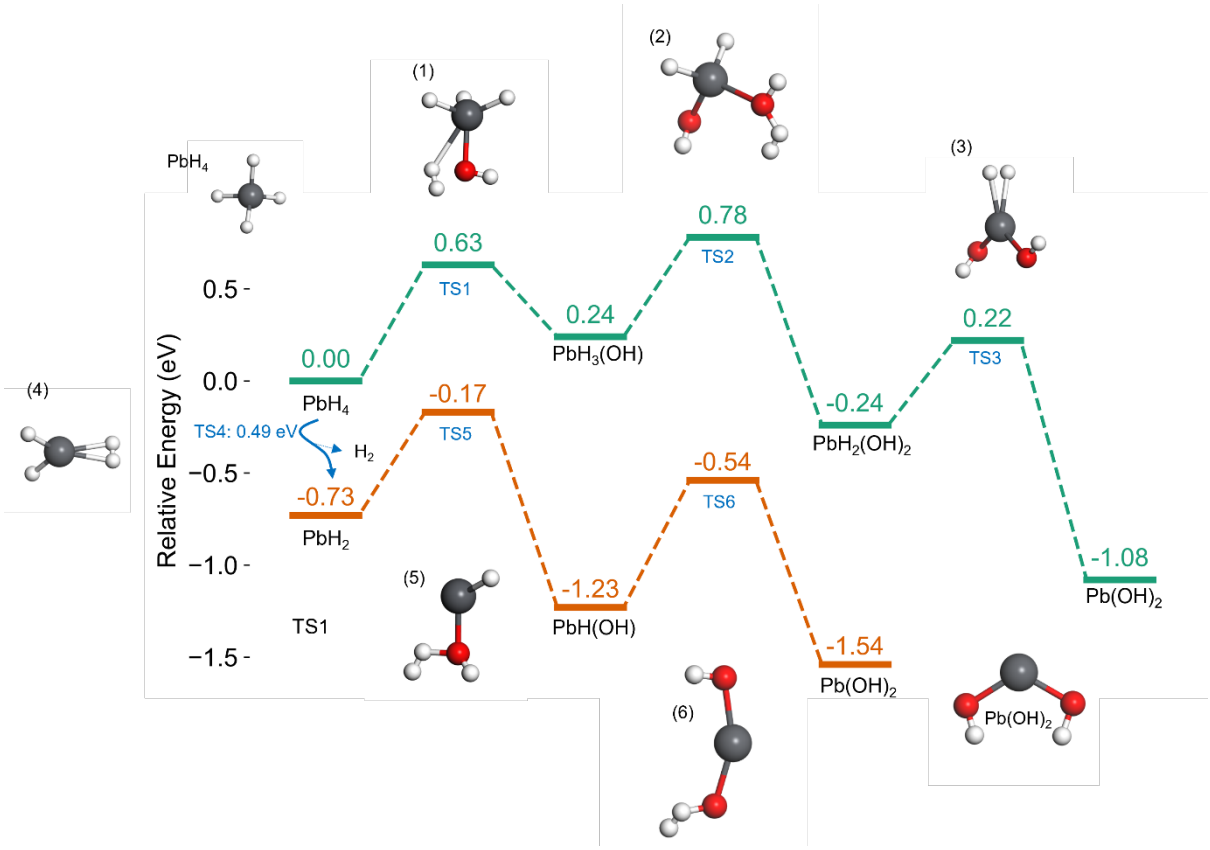

Figure S9. Calculated free-energy profile and key intermediates for the reaction of PbH_4 (green) and PbH_2 (orange) with water leading to $Pb(OH)_2$ formation. All calculations were performed in a 25 Å × 25 Å × 25 Å cubic simulation box with implicit solvation (VASPsol, ε = 78.4) to approximate the solution-phase reaction environment. Reaction barriers were obtained using the CI-NEB method.

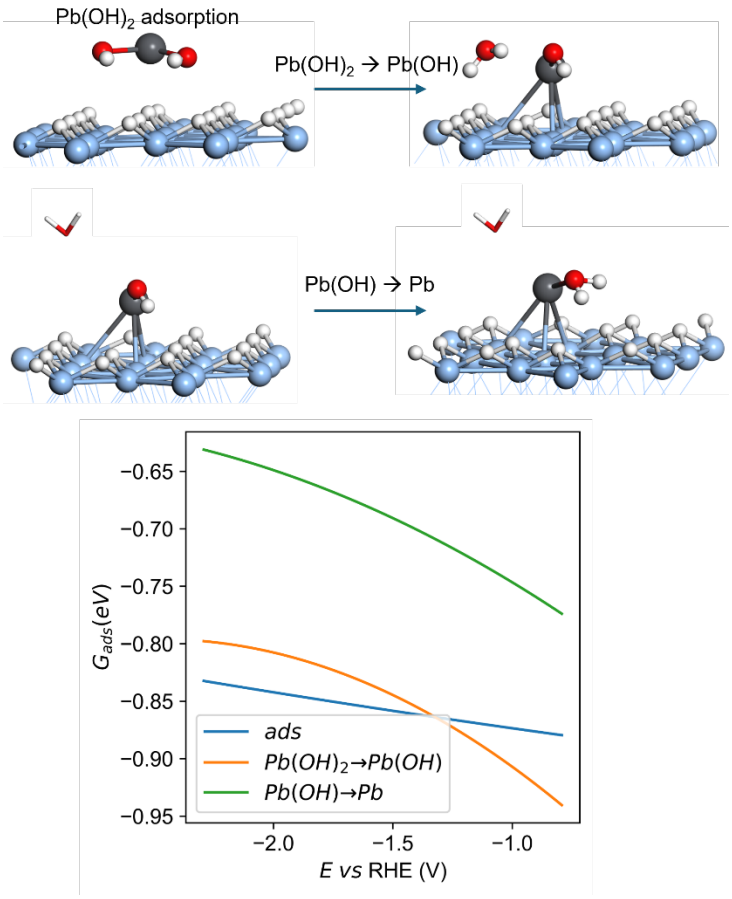

Figure S10. Adsorption structures and calculated free energies for the reduction of $Pb(OH)_2$ on the hydrogen-covered Ag(111) surface. The reduction proceeds via transfer of surface-bound hydrogen atoms rather than direct PCET from solution: $Pb(OH)_2$*/H_{16}-Ag + H* → Pb(OH)*/H_{15}-Ag + H_2O, and Pb(OH)*/H_{15}-Ag + H* → Pb*/H_{14}-Ag + H_2O.

The potential dependence of these hydrogen transfer steps arises from differences in the surface charge distribution between the reactant and product states, which couple differently to the applied electrode potential within the grand canonical DFT framework.

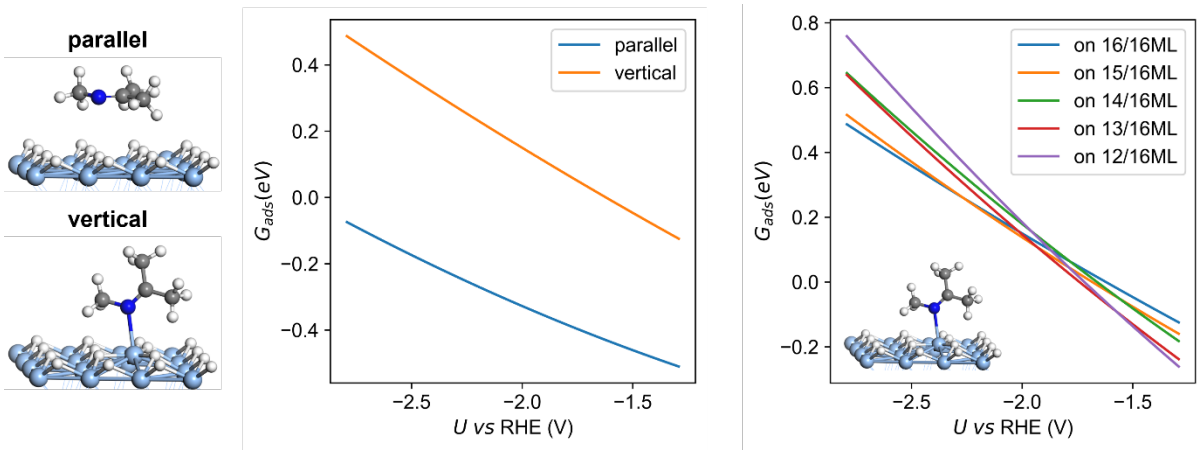

Figure S11. The adsorption of imine on electrified Ag surface: The first part shows the adsorption modes of imine via parallel and vertical ways on the surface; the second part shows the Gibbs adsorption energies of these two modes under different potential conditions; and the third part shows the vertical adsorption energies with potential at several H coverage from 16/16ML to 12/16ML.

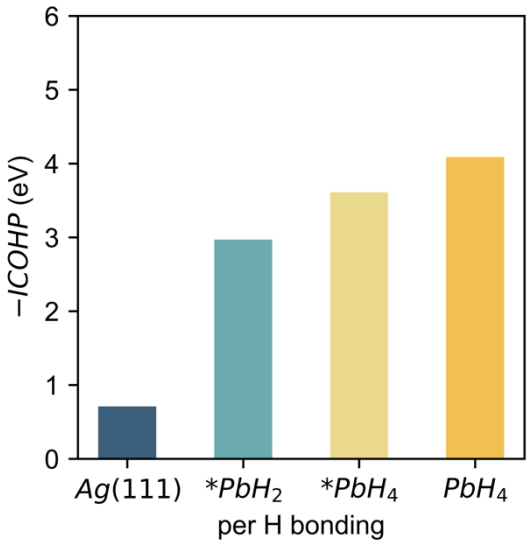

Figure S12. Pb-H bond strength in PbH_2, PbH_4 on the surface, and PbH_4 in the solution illustrated by the Integrated crystal orbital Hamilton population (ICOHP).

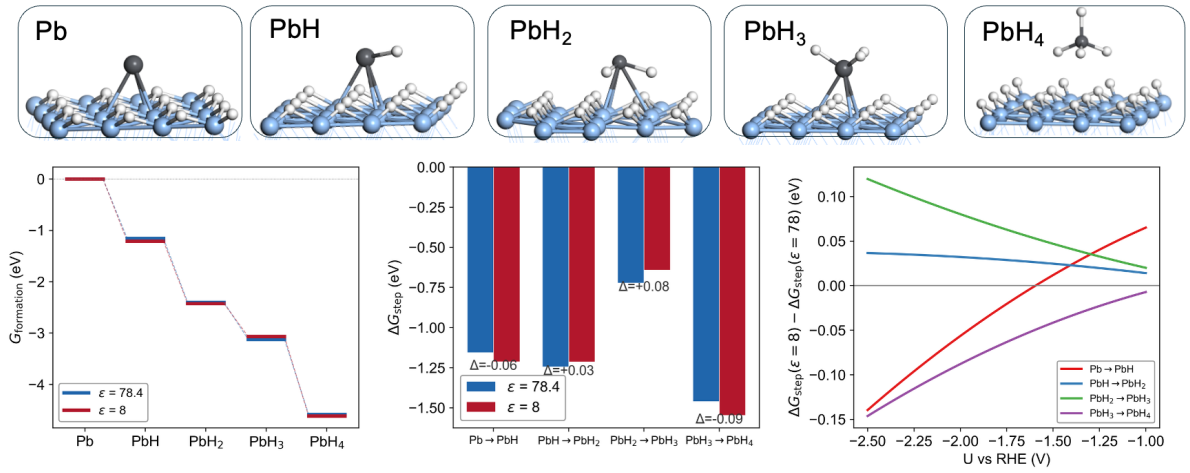

Figure S13. Sensitivity test of the implicit solvation dielectric constant on PbH_n formation energetics. Top: optimized structures of Pb, PbH, PbH_2, PbH_3 adsorbed on the H-covered Ag(111) surface and PbH_4 in the solution phase after desorption. Bottom: (a) cumulative formation energy diagram at U = −2 V vs RHE, comparing ε = 78.4 (blue) and ε = 8 (red); (b) step formation energies at U = −2 V vs RHE with differences (Δ) labeled for each step; (c) potential dependence of the difference in step formation energies between ε = 8 and ε = 78.4 across the experimental potential range.